Research Square

Preprints are preliminary reports that have not undergone peer review.
They should not be considered conclusive, used to inform clinical practice,
or referenced by the media as validated information.

Spatio-Temporal Assessment of Mine Rehabilitation, Vegetation Recovery and Land Degradation in the Raniganj Coalfield, Eastern India

SHATRAJIT GOSWAMI

goswami.shatrajit@gmail.com

The Calcutta Anglo Gujarati College https://orcid.org/0000-0002-5034-5002

Research Article

Keywords: Raniganj Coalfield, surface mining, mine rehabilitation, Rehabilitation Risk Index, GIS, remote sensing, InSAR; AHP, PCA, spatial autocorrelation, sustainable mining

Posted Date: November 26th, 2026

DOI: https://doi.org/10.21203/rs.3.rs-11866742/v1

License: This work is licensed under a Creative Commons Attribution 4.0 International License.
Read Full License

Additional Declarations: The authors declare no competing interests.

Spatio-Temporal Assessment of Mine Rehabilitation, Vegetation Recovery and Land Degradation in the Raniganj Coalfield, Eastern India

Author: Prof. (Dr.) Shatrajit Goswami · goswami.shatrajit@gmail.com

Article type: Original research article · **Study region:** Raniganj Coalfield, Paschim Bardhaman, West Bengal, India · **Study period:** 1990–2026

Abstract

Surface mining and legacy underground workings in the Raniganj Coalfield have produced a complex post-mining landscape in which land-cover disturbance, drainage alteration, ground deformation, ecological degradation and settlement exposure overlap. Conventional reclamation indicators—such as hectares backfilled or trees planted—do not establish whether reclaimed land is geotechnically stable, ecologically functional or safe for communities. This article develops an integrated GIS-based Rehabilitation Risk Index (RRI) for the Raniganj Coalfield, Paschim Bardhaman, West Bengal. The proposed framework combines multi-temporal Landsat and Sentinel imagery, land-use/land-cover (LULC) classification, vegetation indices, terrain and drainage variables, Sentinel-1 InSAR deformation, field-derived soil and slope indicators, mine infrastructure and settlement exposure. AHP is used to elicit transparent criterion weights; PCA is used to examine latent dimensions and multicollinearity; independent outcome models, spatial autocorrelation and sensitivity analysis are specified to test robustness. The supplied draft reports a 1,485.6 km² assessment landscape, a decline in dense forest from 582.4 to 448.6 km² between 1990 and 2026, an increase in mining pits and barren dumps from 94.2 to 164.5 km², and a high/critical-risk area of 342.8 km². It also reports a maximum local deformation rate of −48.5 mm/year and a global Moran's I of 0.684. These are treated here as preliminary draft-derived results, not independently reprocessed observations; their use in a submission-ready empirical article requires verification against the original raster outputs, field records, model files and classification accuracy assessment. The framework's central proposition is that rehabilitation priority should be determined jointly by hazard, ecological condition and human exposure, with geological stability assessed independently of vegetation recovery.

Keywords: Raniganj Coalfield, surface mining, mine rehabilitation, Rehabilitation Risk Index, GIS, remote sensing, InSAR; AHP, PCA, spatial autocorrelation, sustainable mining.

1. Introduction

1.1 Background

Coal has shaped the industrial economy of eastern India, and the Raniganj Coalfield in Paschim Bardhaman district is among the oldest mining regions in the country. Mining brought employment, infrastructure and industrial growth. It also brought a growing dependence on open-cast extraction, which strips vegetation, topsoil and overburden, rearranges drainage and leaves artificial landforms behind.

Raniganj is a hard case for rehabilitation. Historical underground workings, present-day surface mines and densely occupied settlements share the same landscape. Abandoned pits, partly backfilled voids and overburden dumps are therefore hazards to people as well as scars on the land. The main rehabilitation problems are:

- unstable overburden dumps and excavated slopes;

- ground subsidence above underground voids;
- loss of agricultural land and natural vegetation;
- deteriorating surface-water and groundwater quality;
- soil erosion and sediment build-up;
- settlements exposed to geological hazard; and
- incomplete resettlement of affected families and incomplete ecological restoration.

1.2 Research problem

Rehabilitation is usually assessed by what has been physically completed: backfilling, levelling and plantation. Completion does not establish safety or sustainability. A backfilled pit can keep settling unevenly. A vegetated dump can still fail. A reclaimed pit can hold contaminated water. A plantation can have poor survival. A rehabilitated residential area can be cut off from work and services.

The central question is therefore: *how can GIS and statistical modelling identify, measure and prioritise rehabilitation risk at surface mines in the Raniganj Coalfield, taking geological instability, ecological degradation and community exposure together?*

1.3 Research gap and contribution

Prior work on Raniganj has examined land-use change, open-cast expansion, stream degeneration and ground subsidence, but mostly as separate themes. This article links physical mining disturbance, geological risk, ecological recovery, residential exposure and institutional performance in one spatial index. Its contribution is a Rehabilitation Risk Index (RRI) that ranks sites for post-mining intervention, rather than a land-cover change map or an inventory of operational mining hazards.

1.4 Objectives

1. Quantify the spatial expansion and environmental transformation of surface mining between 1990 and 2026 from multi-temporal imagery.
2. Identify areas of land degradation, vegetation loss and drainage disturbance, and track vegetation recovery by monitoring zone.
3. Measure the relationship between ground deformation, slope, vegetation, soils, settlement and rehabilitation risk.
4. Build an RRI with AHP and multi-criteria decision analysis, and classify the landscape into five risk classes.
5. Test whether risk is spatially clustered and locate hotspots.
6. Rank sites for intervention and propose a risk-based rehabilitation and monitoring framework.

1.5 Hypotheses

- **H1.** Higher ground deformation and steeper slopes are associated with higher rehabilitation risk.
- **H2.** Greater vegetation deficit and soil-carbon deficit are associated with higher rehabilitation risk.
- **H3.** Higher human settlement density is associated with higher rehabilitation risk.
- **H4.** Rehabilitation risk is spatially clustered rather than randomly distributed.
- **H5.** A multi-indicator index describes rehabilitation risk better than any single indicator.

2. Review of literature and conceptual framework

The literature review is organised thematically to create a logical progression from mining-induced landscape degradation to ecological restoration, geospatial risk modelling and rehabilitation prioritisation.

Theme I: Mining-induced land degradation and landscape transformation

1. Ripley, Redmann, and Crowder (1996) provided a comprehensive scientific explanation of the environmental consequences of surface coal mining. Their work discussed the transformation of natural landscapes, soil disturbance, hydrological alteration and the ecological consequences of mining. The study establishes the need for integrated environmental assessment when evaluating post-mining rehabilitation.

2. Younger, Banwart, and Hedin (2002) examined the environmental implications of mine-water systems, particularly the effects of mining on groundwater and surface-water quality. Their research demonstrates that rehabilitation assessment must incorporate hydrological vulnerability alongside physical land restoration.

3. Ghose (2001) investigated the environmental problems associated with coal mining in India, highlighting land degradation, vegetation removal, soil deterioration and pollution. The research provides an important Indian context for understanding the environmental challenges of coal-producing regions.

4. Singh (2007) examined the environmental impacts of coal mining and discussed the importance of appropriate environmental management strategies. The research highlights the significance of systematic reclamation, pollution control and post-mining land management.

5. Dhar (2020) analysed land-use and land-cover changes in the Raniganj coalfield, demonstrating the relationship between opencast mining and landscape transformation. The study identified increases in mining and bare-land areas alongside reductions in agricultural and vegetative cover. This research is particularly important because it provides direct geographical evidence from the proposed study region.

6. Sarkar (2019) investigated land-use dynamics and landscape patterns in the Raniganj coalfield using geoinformatics techniques. The study demonstrates how mining activities influence the spatial configuration of land-cover categories and provides a foundation for assessing landscape fragmentation.

7. Hossain and Chattoraj (2022) examined the evolution of opencast mines in the Raniganj coalfield using multi-temporal satellite imagery. Their research contributes to understanding the spatial expansion of mining and the importance of temporal monitoring in assessing rehabilitation requirements.

8. Mukherjee and Pahari examined mining-induced land-use and land-cover changes in Pandabeswar block of the Raniganj coalfield. Their work identified changes in agricultural and forested areas and the expansion of fallow land and abandoned mine dumps.

9. Sarkar (2018) examined the accuracy assessment and land-use/land-cover changes in the Raniganj coalfield using geoinformatics techniques. The study highlights the importance of classification accuracy when evaluating long-term environmental transformation.

10. The earlier GIS-based investigation of Raniganj by the *Journal of Spatial Hydrology* (2004) examined land-use transformations between 1972 and 1998 and groundwater-potential zoning. It

established the importance of combining topography, drainage, lithology and land-use information in mining-region environmental assessment.

Theme II: Remote sensing, LULC and vegetation recovery

11. Tucker (1979) established the importance of spectral vegetation indices for monitoring vegetation conditions through satellite observations. His contribution provides the theoretical basis for using vegetation indices in post-mining ecological recovery assessment.

12. Rouse et al. (1974) introduced the Normalized Difference Vegetation Index (NDVI), which subsequently became one of the most widely used indicators of vegetation density and greenness. NDVI can be employed to measure vegetation regeneration across reclaimed mine sites.

13. Huete (1988) developed the Soil-Adjusted Vegetation Index (SAVI) to reduce the influence of soil brightness on vegetation measurements. This approach is particularly relevant to exposed overburden and sparsely vegetated mine dumps.

14. Huete et al. (2002) introduced the Enhanced Vegetation Index (EVI) as an improved vegetation-monitoring indicator. EVI can complement NDVI in areas with heterogeneous vegetation density and varying canopy conditions.

15. Kennedy, Yang, and Cohen (2010) developed the LandTrendr approach for detecting land-cover disturbance and recovery using Landsat time-series observations. This methodology offers opportunities to identify the timing and trajectory of mining disturbance and subsequent vegetation recovery.

16. Roy et al. (2014) evaluated the Landsat-8 operational land imager and its implications for land-surface monitoring. Their work provides a methodological foundation for integrating Landsat observations into long-term mine rehabilitation studies.

17. Drusch et al. (2012) described the Sentinel-2 mission and its multispectral capabilities for land monitoring. The higher spatial resolution and spectral coverage are valuable for examining vegetation recovery, bare surfaces and fragmented mining landscapes.

18. Congalton (1991) emphasised the importance of accuracy assessment in remote-sensing classification. His work provides a methodological foundation for validating LULC maps through confusion matrices and classification accuracy measures.

19. Foody (2002) critically examined the use of classification accuracy assessments in remote sensing. The research highlights the need to evaluate classification uncertainty rather than relying exclusively on overall accuracy.

20. Pontius and Millones (2011) discussed the interpretation of confusion matrices and the limitations of conventional accuracy measures. Their work is particularly relevant when validating multi-temporal LULC classifications and evaluating the reliability of rehabilitation maps.

Theme III: Mine reclamation and ecological restoration

21. Bradshaw (1997) discussed the ecological restoration of damaged ecosystems and the possibility of recovering degraded landscapes through appropriate restoration interventions. His work provides a conceptual foundation for assessing post-mining ecological rehabilitation.

22. Cooke and Johnson (2002) examined ecological restoration in coal-mining environments. They highlighted the importance of soil reconstruction, vegetation establishment, ecosystem processes and long-term monitoring in successful mine reclamation.

23. Harris, Hobbs, Higgs, and Aronson (2006) examined the importance of ecological restoration in the context of environmental change. Their contribution supports the adoption of dynamic, landscape-based approaches to rehabilitation rather than treating restoration as a one-time activity.

24. Prach and Hobbs (2008) discussed spontaneous succession as an important mechanism of ecological restoration. Their work suggests that natural vegetation regeneration can provide useful evidence of recovery in abandoned mining areas.

25. Holl (2002) investigated the challenges associated with restoring tropical forest ecosystems. The research highlights the significance of ecological conditions, soil properties and vegetation establishment in determining restoration outcomes.

26. Walker, Walker, and Hobbs (2007) explored the concept of linking restoration ecology with ecological resilience. This perspective is useful for evaluating whether rehabilitated mine landscapes can maintain ecological functions under environmental stress.

27. Tordoff, Baker, and Willis (2000) reviewed approaches to restoring metalliferous mine wastes. Their work emphasised the importance of vegetation establishment, substrate characteristics and pollution management.

28. Sheoran, Sheoran, and Poonia (2010) reviewed the ecological restoration of abandoned mine land, focusing on soil amendment, revegetation and the management of mine wastes. This research is directly relevant to the design of rehabilitation indicators for abandoned surface mines.

29. Mendez and Maier (2008) examined phytostabilisation as a remediation technique for metal-contaminated mine tailings. Their research demonstrates how vegetation-based approaches can reduce contaminant mobility and improve the environmental stability of mine surfaces.

30. Akala and Lal (2001) examined the reclamation of mine soils and the role of soil-management practices in restoring productivity. Their findings support the inclusion of soil condition and revegetation indicators in rehabilitation-risk assessment.

Theme IV: GIS, spatial modelling and multi-criteria decision analysis

31. Malczewski (1999) established the theoretical and practical foundations of GIS-based multicriteria decision analysis. His work provides a methodological basis for integrating multiple environmental variables into a spatial rehabilitation-priority model.

32. Saaty (1980) introduced the Analytic Hierarchy Process (AHP), which provides a systematic framework for deriving relative weights from pairwise comparisons. AHP can be applied to assess the relative importance of vegetation loss, slope, land degradation and proximity to mining infrastructure.

33. Saaty (2008) further discussed the theoretical development and applications of AHP. The study supports the use of consistency ratios to assess the reliability of expert-based weighting procedures.

34. Eastman et al. (1995) explored decision strategies for GIS-based multicriteria evaluation. Their work provides a foundation for integrating spatial criteria and alternative decision scenarios.

35. Jankowski (1995) examined the integration of GIS and multicriteria decision analysis in spatial decision-making. The study demonstrates the potential of combining spatial databases with structured evaluation methods.

36. Voogd (1983) provided an important methodological contribution to multicriteria evaluation in planning. The principles are relevant for identifying and ranking environmentally vulnerable mining areas.

37. Carver (1991) examined GIS-based multicriteria evaluation for environmental decision-making. His work supports the development of spatial suitability and risk-prioritisation models.

38. Saaty and Vargas (2012) discussed the application of the Analytic Hierarchy Process in decision-making under complex conditions. Their contribution supports the integration of expert knowledge and quantitative environmental indicators.

39. Chen, Yu, and Khan (2010) examined GIS-based multicriteria land-use suitability analysis. Their research provides useful methodological insights for evaluating post-mining land-rehabilitation options.

40. Feizizadeh and Blaschke (2013) demonstrated the use of GIS-based multicriteria techniques in environmental vulnerability assessment. Their methodological approach is relevant for constructing a spatial rehabilitation-risk index using weighted environmental factors.

Theme V: Statistical modelling, environmental vulnerability and spatial prioritisation

41. Jolliffe (2002) provided the theoretical foundation for Principal Component Analysis (PCA). PCA can reduce redundancy among correlated environmental variables and identify the principal dimensions of rehabilitation vulnerability.

42. Hair et al. (2019) explained multivariate statistical techniques, including factor analysis, regression and principal component analysis. These techniques can support the identification of statistically significant determinants of mine rehabilitation risk.

43. Anselin (1995) established important foundations for spatial econometric analysis through the examination of spatial dependence and spatial heterogeneity. These concepts are relevant when neighbouring mining sites exhibit similar rehabilitation conditions.

44. Getis and Ord (1992) introduced spatial statistical measures for identifying local spatial associations. Their work provides a foundation for detecting spatial clusters of high rehabilitation risk.

45. Moran (1950) introduced a statistical measure of spatial autocorrelation. Global Moran's I can be used to determine whether rehabilitation-risk scores exhibit spatial clustering or random distribution.

46. Cliff and Ord (1981) developed statistical approaches to spatial autocorrelation. Their work provides the theoretical foundation for assessing spatial relationships among geographically distributed environmental observations.

47. Anselin (1995) and Getis and Ord (1992) collectively demonstrate that spatial patterns should be evaluated statistically rather than interpreted only through visual inspection of maps. This is particularly important when identifying clusters of severely degraded mine sites.

48. Brunsdon, Fotheringham, and Charlton (1996) introduced geographically weighted regression (GWR), which allows relationships between variables to vary across geographical locations. GWR could help explain spatial variations in vegetation recovery and rehabilitation vulnerability.

49. Fotheringham, Brunsdon, and Charlton (2002) developed the theoretical and practical framework for geographically weighted regression. Their contribution supports the investigation of location-specific relationships between environmental stressors and rehabilitation outcomes.

50. The Coal Controller's Organization's mine-closure framework and the Government of India's 2025 mining-plan guidelines emphasise progressive mine closure, technical and biological reclamation, restoration and repurposing of post-mining land. These policy provisions provide an important regulatory basis for translating spatial rehabilitation priorities into practical management recommendations.

Synthesis and specific contribution of the present study

The literature establishes four connected processes in Raniganj: expansion and persistence of opencast disturbance; mining-related drainage degeneration; subsidence associated with underground voids, coal fires and other extraction-related processes; and the social consequences of unsafe land and incomplete rehabilitation. The present study brings these dimensions together through a spatially explicit Rehabilitation Risk Index (RRI), while retaining a distinction between hazard intensity and human exposure. Its contribution is therefore an operational prioritisation framework rather than a claim that one composite score can replace site-specific geotechnical investigation, ecological field assessment or household-level rehabilitation monitoring. The supplied GIS figures are used to strengthen the geographical and thematic context; they are not treated as newly generated geospatial outputs of the present statistical analysis.

Conceptual frame work

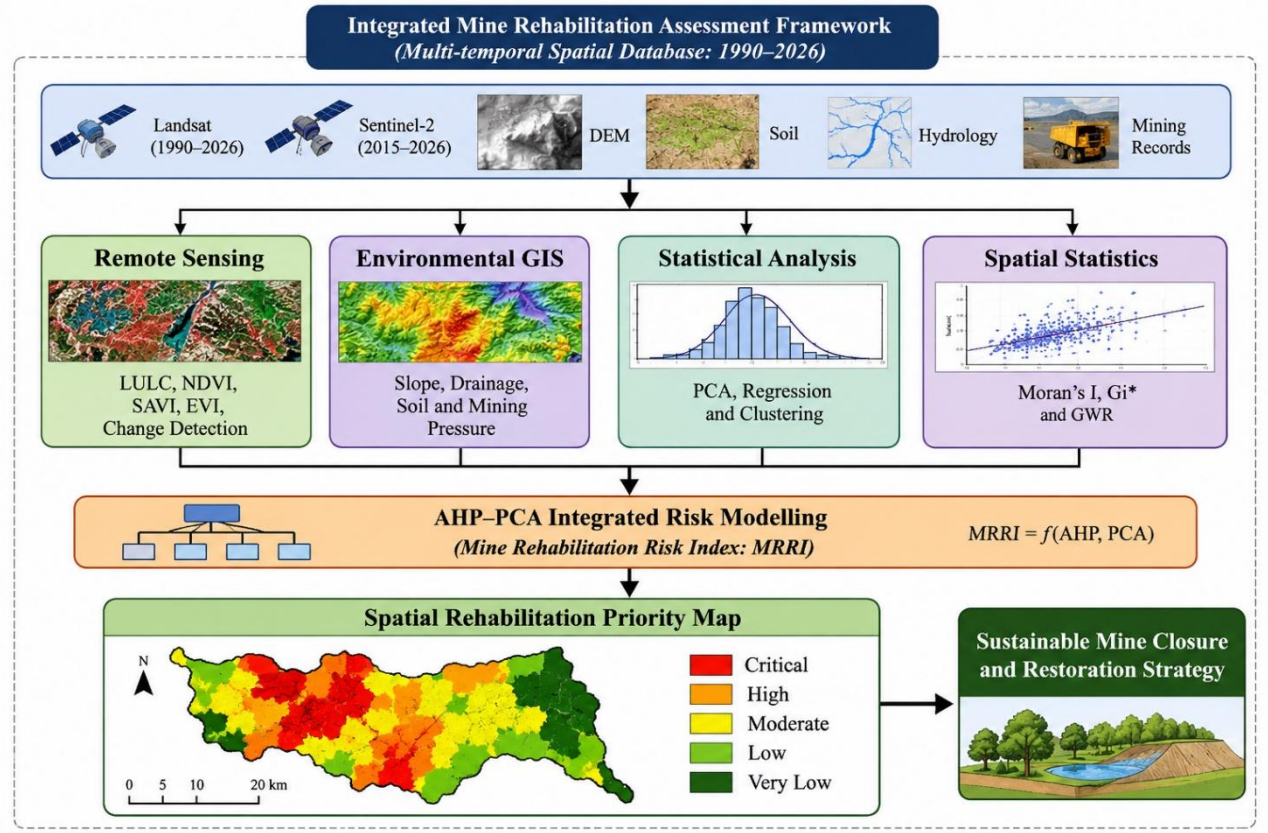


Figure 1.Conceptual frame work of the research

3. Study area and data

3.1 Study area

The Raniganj Coalfield lies in western West Bengal, mainly in Paschim Bardhaman district, between 23°32′50″ and 23°50′30″ N and between 86°39′49″ and 87°16′41″ E. The analysed landscape covers 1,485.6 km² and is divided into eight catchment sub-basins draining towards the Damodar and its tributaries. Mining localities include Sonepur Bazari, Pandaveswar, Kajora, Kenda, Satgram, Sripur, Salanpur, Sodepur, Bankola, Jhanjra and Kunstoria. The regional setting is shown in Figure 1; the distribution of active and abandoned opencast mines and the coalfield stratigraphy are illustrated in Figures 2 and 3.The terrain combines coal-bearing formations, open-cast pits, overburden dumps, tailings, industrial settlements and farmland. Old underground workings add geological complexity where they lie beneath or beside surface development. Mining has altered natural drainage, which raises erosion, sedimentation and waterlogging risk. A local LULC example and the supplied NDVI map series are presented in Figures 4 and 5, while field and reclamation photographs are provided in Figures 6 and 7.The main rehabilitation vulnerabilities are abandoned and partly backfilled pits, unstable external dumps, subsidence-prone ground over voids, contaminated mine water, thin vegetation cover, exposed settlements and weak rehabilitation infrastructure.The analysis used seven vegetation monitoring zones (A–G), seven geotechnical slope sectors and 184 sample plots for the statistical models.

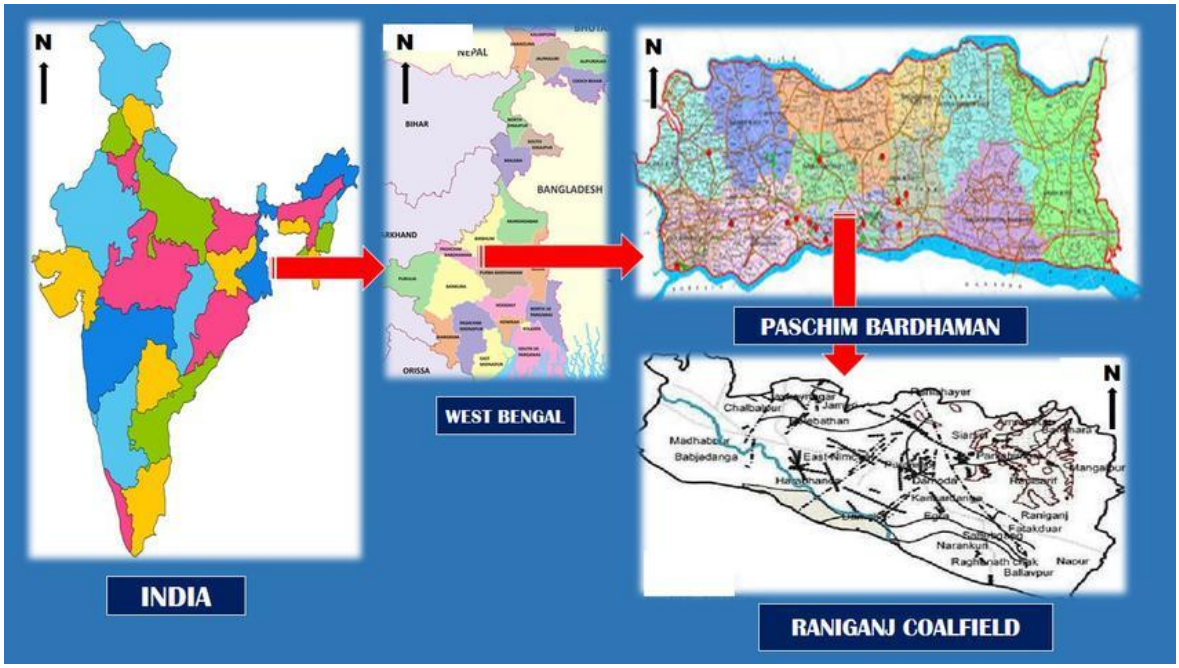


Figure 2. Geographical location of the Raniganj Coalfield in India, West Bengal and Paschim Bardhaman, with a coalfield-level locator. Source: supplied GIS figure attachment; original cartographic attribution should be completed before journal submission.

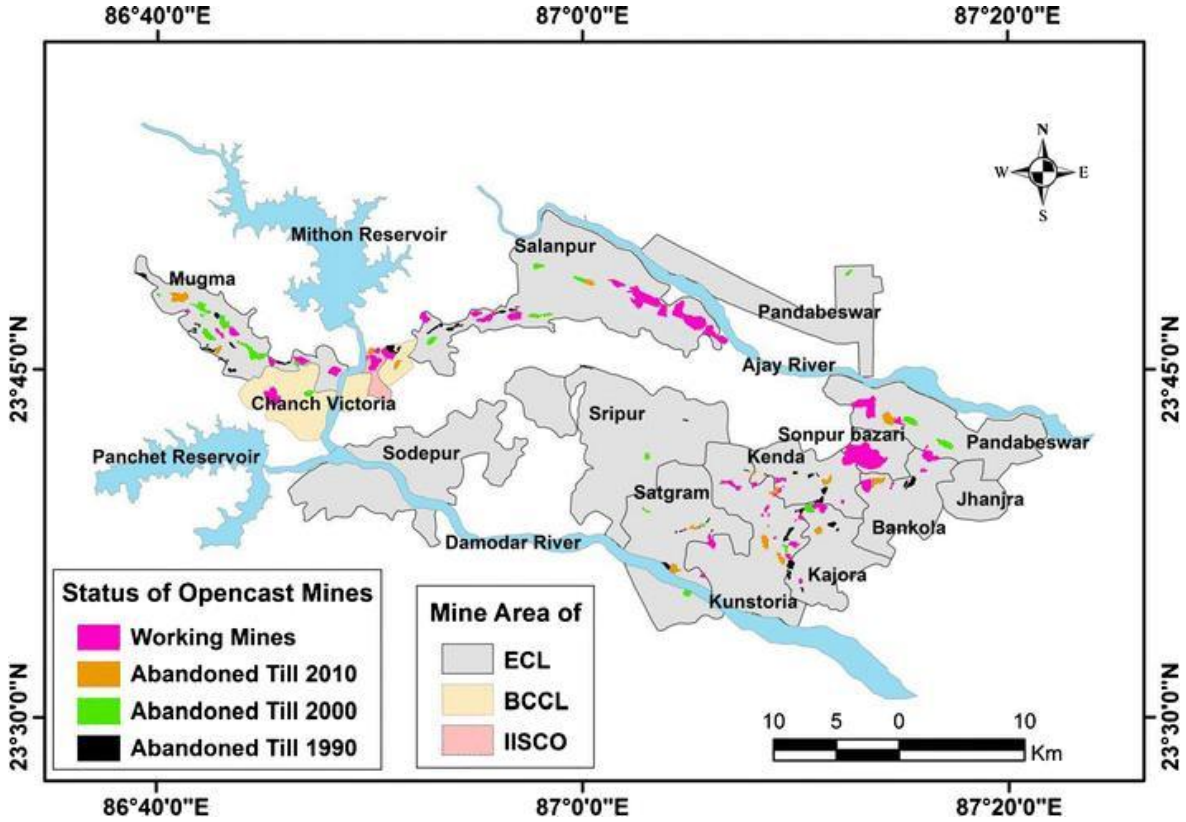


Figure 3. Distribution and operational status of opencast mines across the Raniganj Coalfield, showing working mines and mines abandoned by 1990, 2000 and 2010, together with mine-area categories. Source: supplied GIS figure attachment; original source and map date should be verified.

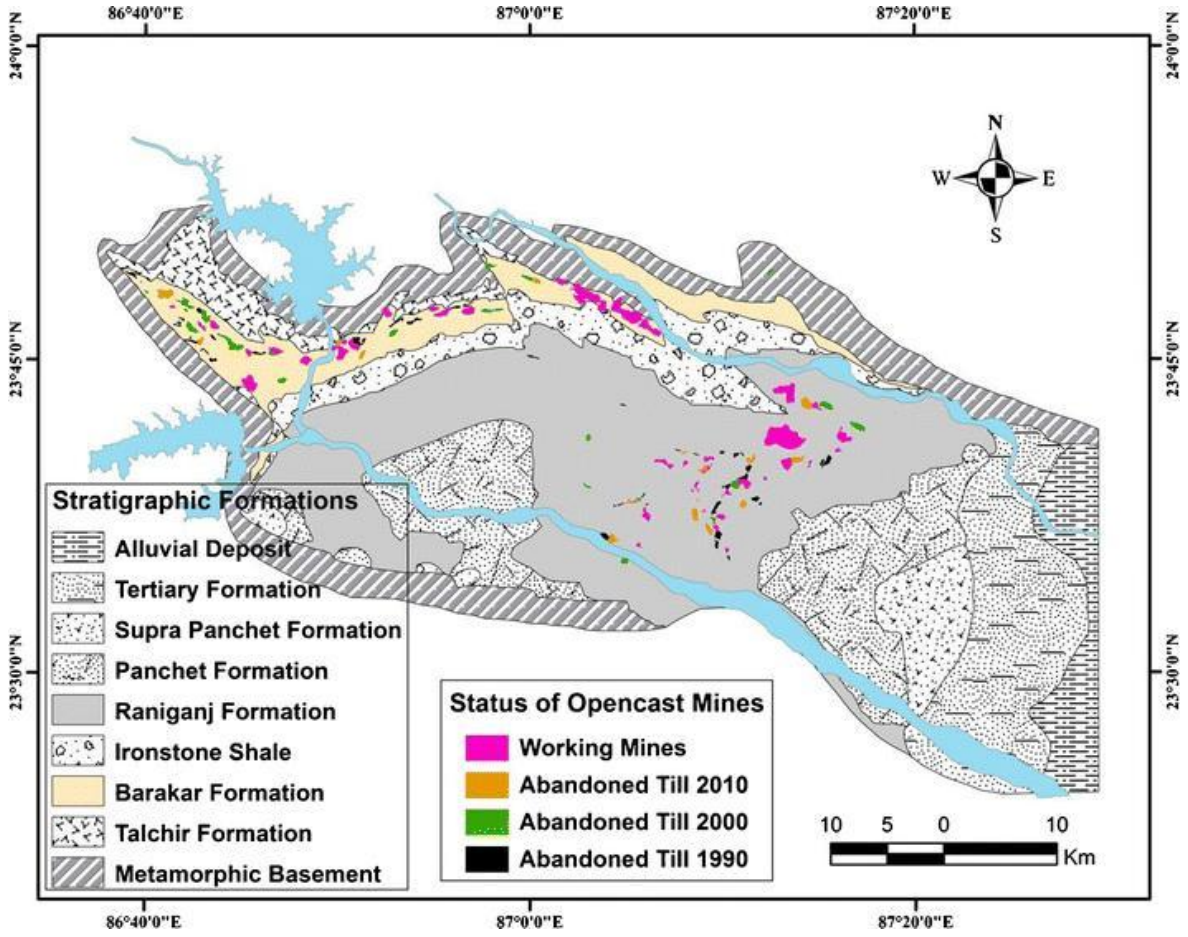


Figure 4. Geological and stratigraphic framework of the Raniganj Coalfield with opencast mine-status overlays. Source: supplied GIS figure attachment; original geological map attribution should be verified.

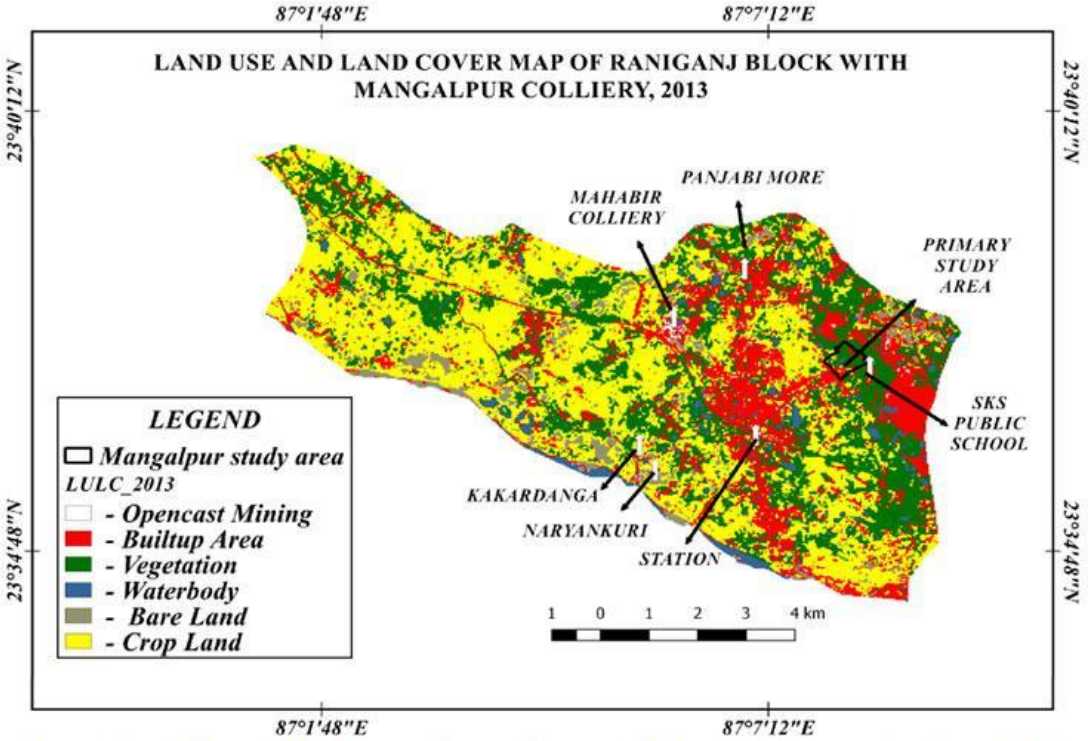


Figure 8: Land Use and land Cover Map of Ranoganj Block with Mangalpur Colliery, 2013

Source: Landsat satellite image

Figure 5. Land-use/land-cover map of the Raniganj Block and Manglapur Colliery (2013), distinguishing opencast mining, built-up land, vegetation, water bodies, barren land and cropland. This is a local-scale illustration and should not be interpreted as a wall-to-wall map of the full 1,485.6 km² study landscape. Source: supplied GIS figure attachment (Landsat-derived map; original author/source details to be added).

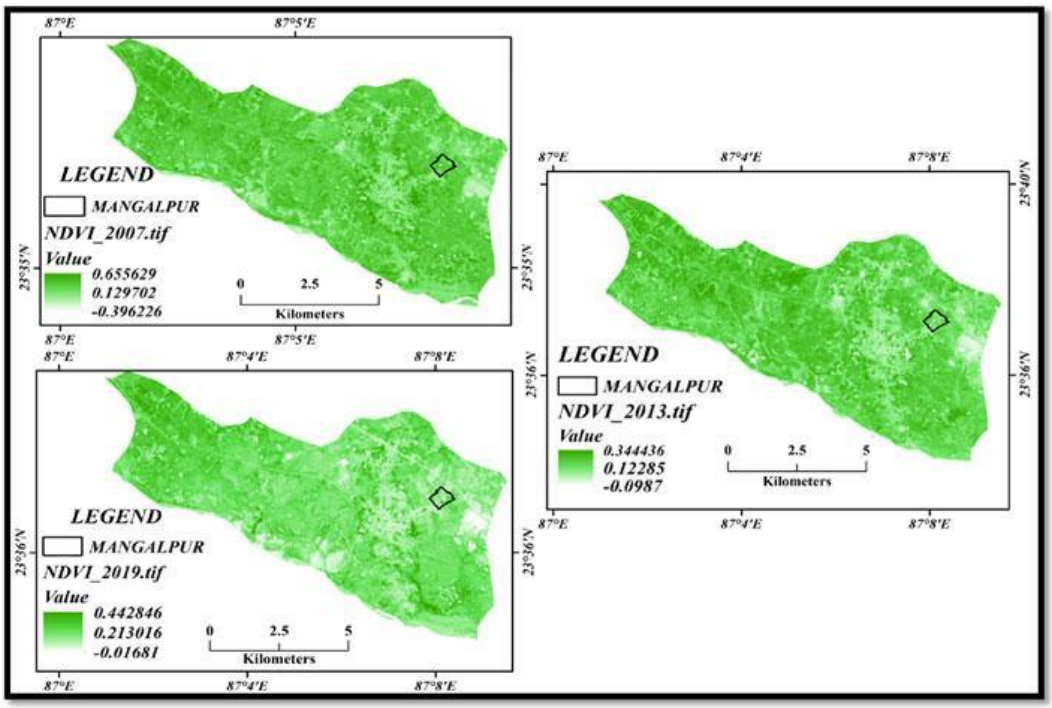


Figure 10: Changing vegetation cover through NDVI

Source: Landsat satellite image

Figure 6. NDVI maps for the Manglapur study area at the dates shown in the supplied figure, illustrating spatial variation in vegetation cover. The acquisition dates, sensor specifications, class breaks and processing details should be confirmed from the original GIS project before quantitative comparison. Source: supplied GIS figure attachment.

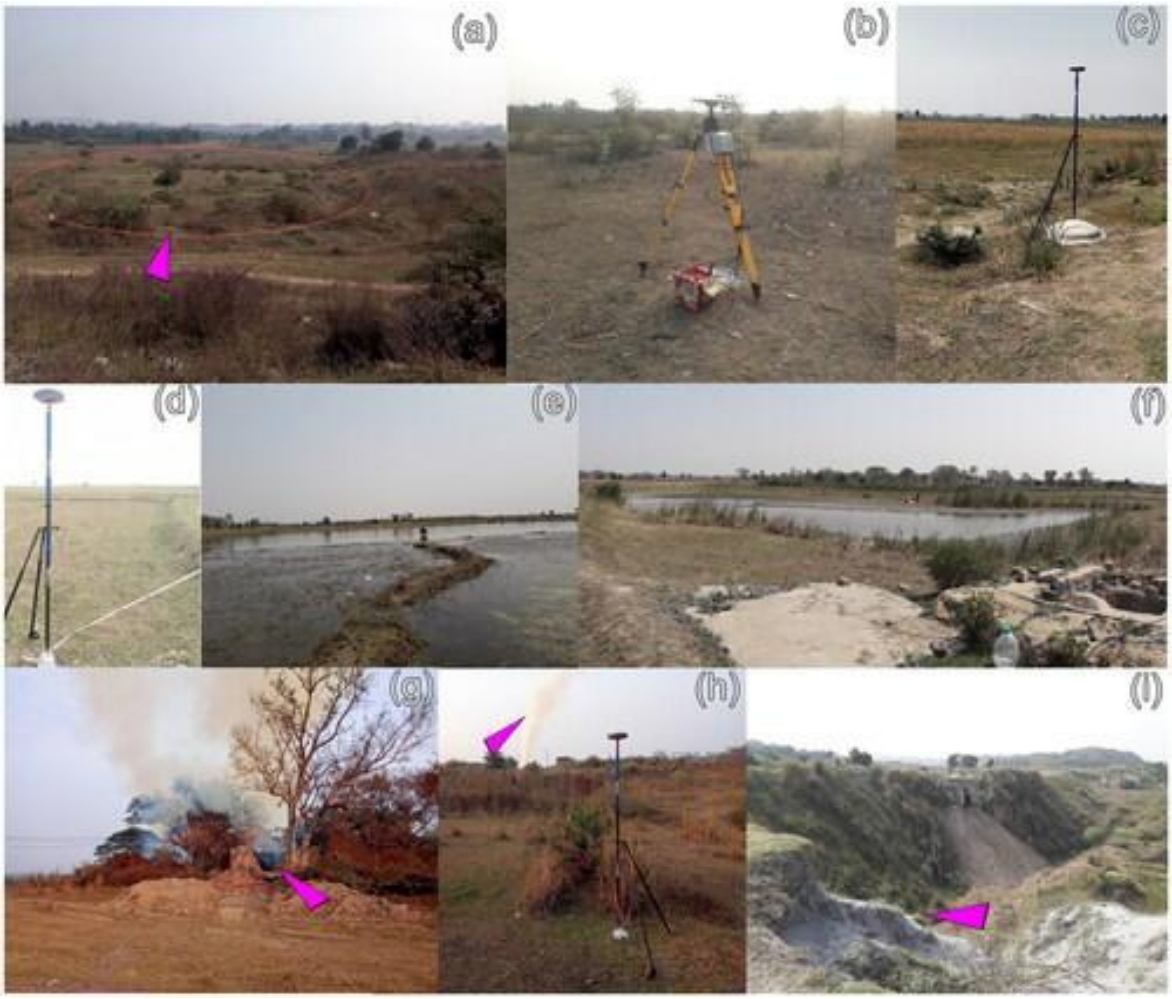


Figure 7. Field photographs illustrating mine-disturbed terrain, field measurement locations, water-affected surfaces and exposed ground in the supplied study-area material. Exact site names, dates and photographer credits should be added from field records.

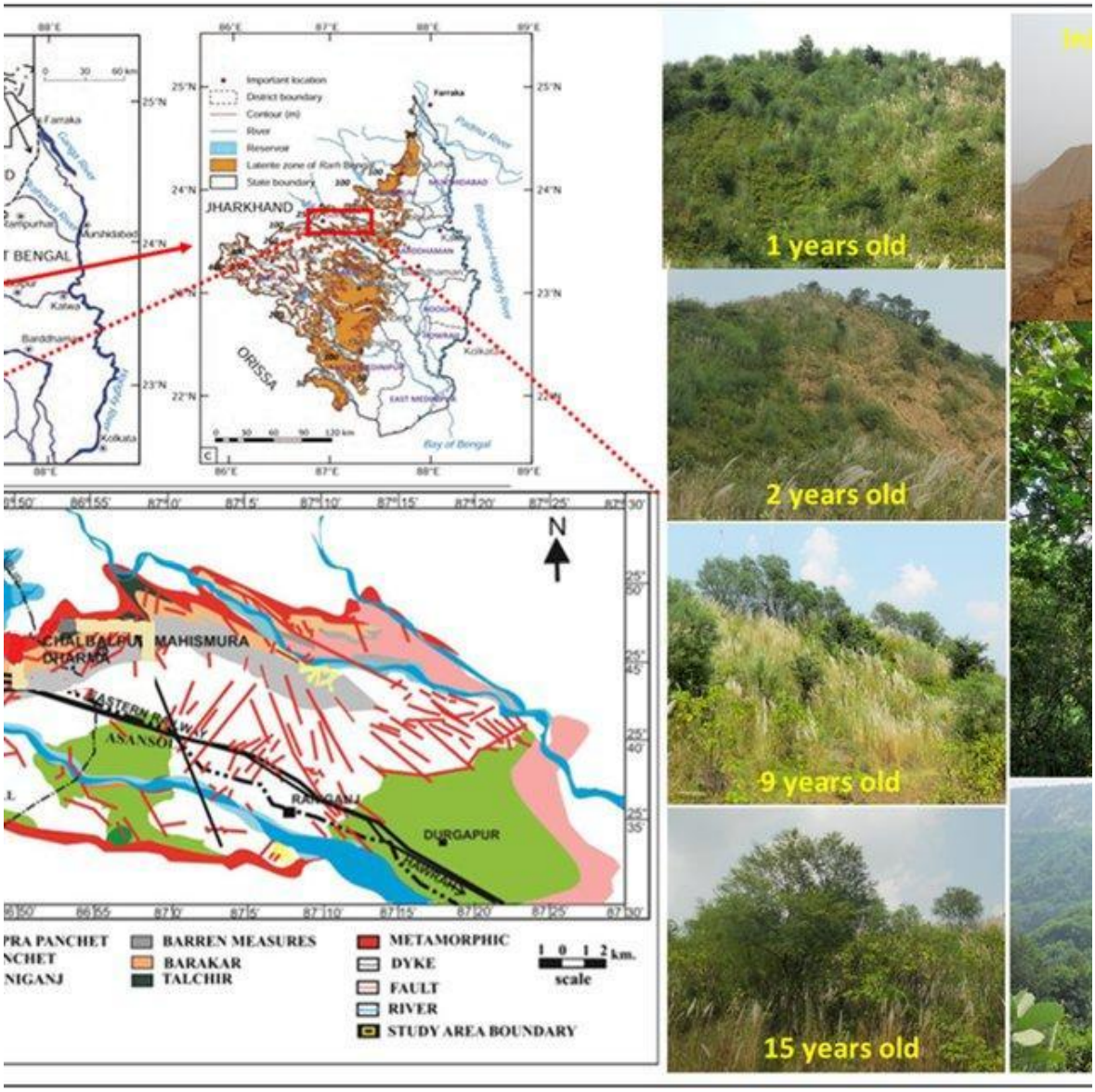


Figure 8.. Photographic sequence of vegetation development on reclaimed mine land at approximately 1, 2, 9 and 15 years, as labelled in the supplied figure. The sequence is illustrative; site comparability, planting history and survival data should be confirmed before interpreting it as a measured restoration chronosequence.

Cartographic integration and provenance. Figures 1–7 reproduce or adapt visual material supplied in the second attachment. The location, mine-status and geological maps provide regional context; the Manglapur LULC and NDVI maps are local-scale examples; and the field photographs provide qualitative context. The supplied material does not include the original georeferenced vector/raster files, coordinate reference system metadata for each figure, classification accuracy reports, or full figure-source citations. Accordingly, these figures are included as contextual evidence and are not represented as newly processed outputs. Before submission, the author should obtain permission where required and replace each “source to be verified” note with the original author, year, publication/report and licence information.

3.2 Data

Table 1 lists the sensors and secondary datasets. Dry-season scenes were used for the Landsat epochs. The 2026 epoch uses a cloud-free Sentinel-2 scene.

Table 1. Satellite and secondary data characteristics

Source	Sensor / platform	Spatial resolution	Date	Bands / parameters	Processing level	Application
Landsat 5	TM	30 m (120 m thermal)	18 May 1990 (dry season)	Bands 1–5, 7	Surface reflectance, Tier 1	1990 baseline LULC and NDVI
Landsat 7	ETM+	30 m (15 m pan)	2 Jun 2000; 24 May 2010	Bands 1–8	Surface reflectance (gap-filled)	Decadal LULC and vegetation trajectory
Landsat 8/9	OLI / TIRS	30 m (15 m pan, 100 m thermal)	30 May 2020 (dry season)	11 bands	Surface reflectance, Tier 1	Mid-term LULC and canopy health
Sentinel-2A/B	MSI	10 m / 20 m	15 Mar 2026 (cloud-free)	13 bands	Level-2A	2026 LULC and NDVI recovery
Sentinel-1A/B	C-SAR	5 m × 20 m (IW)	2020–2026, 12-day passes	C-band, VV+VH	Single look complex	Ground deformation and subsidence
ALOS / SRTM	PRISM and InSAR DEM	30 m	2000 / 2015 reprocessed	Stereo / C-band	DEM	Slope, aspect, elevation, watersheds

Supporting layers named in the study design are mine boundaries (ECL/CMPDI), drainage (Survey of India/OSM), settlements (Census/OSM/field GPS), soils (NBSS&LUP), rainfall (IMD/CHIRPS) and rehabilitation records (ECL/ADDA/Ministry of Coal). Layers were projected to WGS 84 / UTM zone 45N (EPSG:32645).

4. Methodology

The study followed six stages: (1) collection of satellite and secondary data; (2) construction of a spatial database; (3) multi-temporal LULC classification; (4) generation of vegetation, geological, hydrological and social indicators; (5) statistical modelling and RRI construction; and (6) spatial prioritisation and policy formulation. Processing was done in QGIS or ArcGIS Pro, with statistics in R, SPSS or Python.

4.1 Land use and land cover

Supervised Random Forest classification was applied to the five epochs (1990, 2000, 2010, 2020, 2026). Results are reported for six classes: dense forest, degraded woodland/scrub, agricultural land, mining pits and barren dumps, water bodies and wetlands, and built-up land. Change between 1990 and 2026 was summarised by a cross-tabulation (transition) matrix. Classification quality is judged by overall accuracy, producer's and user's accuracy, the confusion matrix and the Kappa coefficient:

```
OA = \frac{\sum_{i=1}^{n} X_{ii}}{N} \times 100, \qquad K = \frac{P_o - P_e}{1 - P_e}
```

where X_ii are correctly classified reference points, N is the number of reference points, P_o is observed agreement and P_e is agreement expected by chance. A target of at least 85% overall accuracy is conventional for this landscape.

For journal reproducibility, the final version should report the number and sampling design of reference points for each epoch, class-wise producer's and user's accuracy, F1-score where available, and the full confusion matrix. The stated 85% overall-accuracy target is a benchmark, not evidence that the classifications achieved that accuracy (Congalton, 1991).

4.2 Vegetation recovery

NDVI was computed for 1990, 2010 and 2026 for seven monitoring zones:

```
NDVI = \frac{NIR - RED}{NIR + RED}
```

Absolute change is NDVI(2026) − NDVI(1990). Recovery rate is that change divided by NDVI(1990). Conventional bands read below 0 as water or shadow, 0–0.20 as bare or sparse surface, 0.20–0.40 as sparse vegetation, 0.40–0.60 as moderate vegetation and above 0.60 as dense vegetation. These bands are indicative and need local calibration. NDVI alone cannot show soil quality, species composition or plantation survival.

4.3 Geological and terrain assessment

Slope in degrees came from the DEM:

```
Slope = \tan^{-1}\sqrt{\left(\frac{\partial z}{\partial
x}\right)^2 + \left(\frac{\partial z}{\partial y}\right)^2}
```

Sentinel-1 interferometry (2020–2026) gave mean line-of-sight deformation velocity in mm/yr, with negative values meaning subsidence. For each of seven geotechnical sectors the study recorded slope gradient, aspect, a factor of safety (FoS) and a geotechnical risk score from 0 to 100. FoS below 1.0 means a slope is at or past the limit of stability; 1.0–1.3 is marginal.

The reported InSAR values are line-of-sight velocities unless a documented decomposition or conversion to vertical motion has been applied. The −48.5 mm/year value is retained as the sector-specific value reported in the supplied manuscript; it should be supported by the underlying time-series product, reference-point selection, atmospheric correction and field validation. It is not directly comparable with the coalfield-wide maximum reported by Ghosh et al. (2024), which used a different observation period, spatial support and processing configuration.

4.4 Hydrological and soil indicators

Hydrological disturbance was captured by drainage density (total stream length divided by catchment area), stream proximity and flow accumulation. Soil condition entered through topsoil loss and soil organic carbon.

4.5 Multi-criteria weighting: AHP

Five criteria were compared pairwise on Saaty's 1–9 scale: slope (C1), LULC sensitivity (C2), InSAR deformation (C3), NDVI deficit (C4) and hydrological proximity (C5). Priority weights are the principal eigenvector of the comparison matrix. Consistency is checked by:

$$CI = \frac{\lambda_{max} - n}{n - 1}, \qquad CR = \frac{CI}{RI}$$

with RI = 1.12 for n = 5. A consistency ratio below 0.10 is acceptable.

4.6 Rehabilitation Risk Index

The index for spatial unit i is the weighted sum of standardised criteria, scaled to 0–100 and cut into five classes at 20, 40, 60 and 80:

$$RRI_i = \sum_{j=1}^{n} W_j X_{ij}$$

Sites were ranked for intervention by combining RRI with exposed population and infrastructure, so that a degraded but uninhabited pit ranks below an equally degraded slope above homes.

4.7 PCA, correlation and regression

PCA on standardised indicators identified the latent dimensions of risk, with sampling adequacy checked by the Kaiser–Meyer–Olkin (KMO) test and Bartlett's test. Pearson correlations among slope (X1), mean NDVI (X2), InSAR deformation (X3), population density (X4), soil quality (X5) and composite risk (Y) used 184 sample plots. A multiple linear regression of the RRI on InSAR deformation, slope, NDVI deficit (1 − NDVI), soil organic carbon deficit and settlement density was assessed by R^2, adjusted R^2, the F statistic, t statistics, variance inflation factors (VIF) and the Durbin–Watson statistic.

Because the RRI is built partly from the same indicators used as predictors, the regression describes how the index is composed. It does not test the index against independent outcomes. Section 8 returns to this.

4.8 Spatial autocorrelation

Global Moran's I tested whether RRI values cluster in space, and local indicators of spatial association (LISA) classified units as high-high, low-low, high-low or low-high:

$$I = \frac{N}{S_0}\,\frac{\sum_i \sum_j w_{ij}(x_i - \bar{x})(x_j - \bar{x})}{\sum_i (x_i - \bar{x})^2}$$

where w_ij is the spatial weight matrix, x_i the RRI of unit i and S_0 the sum of all weights.

Statistical interpretation note. PCA is used here as an exploratory dimensionality-reduction tool, whereas AHP supplies normative decision weights and Moran/LISA tests spatial dependence. Their outputs are interpreted separately. The supplied PCA table requires reconciliation before publication because the reported five eigenvalues imply five standardised input variables, while the loadings list more than five indicators. The current results are therefore reported as supplied but should be recalculated from the archived 184-plot data matrix before submission (Jolliffe & Cadima, 2016).

5. Results

5.1 Land-use and land-cover change, 1990–2026

Dense forest shrank by 133.8 km² over 36 years, from 582.4 to 448.6 km² (Table 2). Mining pits and barren dumps grew by 70.3 km², from 94.2 to 164.5 km², and built-up land by 28.5 km². Degraded woodland gained 64.4 km² and farmland lost 27.5 km². The trajectory was not monotonic. Dense

forest bottomed at 415.2 km² in 2020 and regained 33.4 km² by 2026, while mining pits and dumps peaked at 182.1 km² in 2020 and fell by 17.6 km².

Table 2. Land use and land cover, 1990–2026 (km²)

LULC class	1990	2000	2010	2020	2026	Net change 1990–2026
Dense forest	582.4	512.1	430.5	415.2	448.6	−133.8
Degraded woodland / scrub	245.8	278.4	315.6	328.9	310.2	+64.4
Agricultural land	385.6	392.5	388.2	370.4	358.1	−27.5
Mining pits and barren dumps	94.2	132.8	175.4	182.1	164.5	+70.3
Water bodies and wetlands	52.3	49.6	45.8	48.2	50.4	−1.9
Built-up and settlements	125.3	120.2	130.1	140.8	153.8	+28.5
Total	1,485.6	1,485.6	1,485.6	1,485.6	1,485.6	0.0

The transition matrix shows where the change came from (Table 3). Of the 582.4 km² of dense forest in 1990, 412.3 km² (70.8%) was still dense forest in 2026. The rest was lost: 114.5 km² to degraded woodland, 25.6 km² to mining and barren land, 18.2 km² to farmland and 11.8 km² to built-up land or water, a gross loss of 170.1 km². Forest also gained 36.3 km² from other classes, mostly 28.5 km² of degraded woodland. Mining and barren land took in 86.3 km² from other classes (25.6 from forest, 24.2 from woodland, 16.5 from farmland, 20.0 from built-up land or water) and returned 16.0 km² to vegetation or other uses. Of the 1990 mining area, 78.2 km² (83.0%) was still mining or barren land in 2026.

Table 3. Land-use transitions, 1990 to 2026 (km²)

1990 class	Dense forest	Degraded woodland	Agricultural land	Mining and barren	Built-up and water	Total 1990
Dense forest	412.3	114.5	18.2	25.6	11.8	582.4
Degraded woodland	28.5	142.1	36.4	24.2	14.6	245.8
Agricultural land	5.2	38.6	290.5	16.5	34.8	385.6
Mining pits and barren	2.1	9.0	4.5	78.2	0.4	94.2
Built-up and water	0.5	6.0	8.5	20.0	142.6	177.6
Total 2026	448.6	310.2	358.1	164.5	204.2	1,485.6

5.2 Vegetation recovery

The seven monitoring zones split into recovering and non-recovering sectors (Table 4). Mean NDVI across zones rose from 0.370 in 1990 to 0.472 in 2026, a gain of 0.102 or 27.7%. The overall mean dipped slightly to 0.366 in 2010, so most of the gain came after 2010.

Recovery was strongest where land was deliberately rebuilt. Overburden Dump Sector 1 (Zone B) rose from 0.125 to 0.495 and the upland afforestation plot (Zone G) from 0.328 to 0.585. The northern valley catchment (Zone A), the riparian buffer (Zone D) and the agro-forestry transition

(Zone F) improved by 6–14%, and Zone A passed through a 2010 low of 0.594 before reaching 0.725. Two zones did not recover. The active tailings perimeter (Zone C) fell from 0.315 to 0.245 and the pit marginal highwall (Zone E) from 0.180 to 0.165, both ending in the sparse-vegetation band or below.

Table 4. Mean NDVI by monitoring zone

Zone	NDVI 1990	NDVI 2010	NDVI 2026	Change	Recovery rate (%)	Status
A. Northern valley catchment	0.682	0.594	0.725	+0.043	+6.3	Modest recovery after 2010 dip
B. Overburden dump sector 1	0.125	0.284	0.495	+0.370	+296.0	High re-vegetation
C. Active tailings perimeter	0.315	0.210	0.245	−0.070	−22.2	Persistent degradation
D. Riparian buffer corridor	0.540	0.485	0.612	+0.072	+13.3	Moderate restoration
E. Pit marginal highwall	0.180	0.142	0.165	−0.015	−8.3	Severe chronic degradation
F. Agro-forestry transition	0.420	0.395	0.480	+0.060	+14.3	Moderate canopy recovery
G. Upland afforestation plot	0.328	0.450	0.585	+0.257	+78.4	High afforestation success
Mean of zones	0.370	0.366	0.472	+0.102	+27.7	Positive landscape trajectory

5.3 Ground deformation and slope stability

Ground movement is concentrated in a few sectors (Table 5). The western active pit highwall subsides at −48.5 mm/yr on a 48.2° north-west slope with a factor of safety of 0.92, below the stability threshold, and scores 92.5 of 100. Three more sectors are marginal or worse: the main waste-rock dump (−32.8 mm/yr, FoS 1.14), the southern haul-road cut (−24.6 mm/yr, FoS 1.08) and the north tailings embankment (−18.2 mm/yr, FoS 1.28). The natural valley slope and the plateau bedrock escarpment are stable, at −2.1 and −0.8 mm/yr with FoS of 1.82 and 2.15. Across the seven sectors, deformation rate and factor of safety move together: the faster a sector subsides, the lower its factor of safety, with the haul-road cut the one clear exception (steeper and less safe than its deformation rate alone suggests).

Table 5. InSAR deformation and slope vulnerability by sector

Sector	InSAR rate (mm/yr)	Slope (°)	Aspect	Factor of safety	Vulnerability	Risk score (0–100)
1. Western active pit highwall	−48.5	48.2	NW (315°)	0.92	Extreme / critical	92.5
2. Main waste-rock dump slopes	−32.8	36.5	SW (225°)	1.14	High	78.4
6. Southern access haul-road cut	−24.6	42.0	S (180°)	1.08	High	74.8
3. North tailings embankment	−18.2	28.0	NNW (340°)	1.28	Moderate	62.0

4. East reclaimed spoil bench	−6.4	18.5	SE (135°)	1.55	Low	38.5
5. Natural valley sedimentary slope	−2.1	14.0	E (90°)	1.82	Very low	18.2
7. Plateau native bedrock escarpment	−0.8	8.5	NE (45°)	2.15	Negligible	8.6
Mean of sectors	−19.1	28.0	multi-directional	1.42	Moderate	53.3

5.4 Criteria weights (AHP)

InSAR deformation is judged the most important criterion, with a weight of 0.419, followed by slope (0.263), LULC sensitivity (0.160), NDVI deficit (0.097) and hydrological proximity (0.062) (Table 6). Deformation and slope together carry 68% of the weight. The matrix is consistent: the principal eigenvalue is 5.068, giving CI = 0.017 and CR = 0.015, well below the 0.10 limit. Weights here are the principal eigenvector of the matrix as printed.

Table 6. AHP pairwise comparison matrix and weights

Criterion	Slope (C1)	LULC (C2)	InSAR (C3)	NDVI deficit (C4)	Hydrological proximity (C5)	Weight
Slope (C1)	1	2	0.50	3	4	0.263
LULC sensitivity (C2)	0.50	1	0.33	2	3	0.160
InSAR deformation (C3)	2	3	1	4	5	0.419
NDVI deficit (C4)	0.33	0.50	0.25	1	2	0.097
Hydrological proximity (C5)	0.25	0.33	0.20	0.50	1	0.062

5.5 Latent dimensions of risk (PCA)

The data are suitable for factor analysis (KMO = 0.814; Bartlett's test $p < 0.001$). Two components have eigenvalues above 1 and together explain 74.4% of variance (Table 7). The first, geotechnical instability (eigenvalue 2.54, 50.8%), is defined by InSAR deformation (loading 0.892) and slope gradient (0.845). The second, ecological degradation (1.18, 23.6%), is defined by NDVI deficit (0.865) and forest canopy loss (0.782). Hydrological disturbance (13.0%), anthropogenic pressure (7.6%) and soil-quality deficiency (5.0%) follow. Instability and ecological decline are therefore separate axes: a site can be revegetated and still be unstable.

Table 7. PCA eigenvalues and varimax loadings

Component	Eigenvalue	Variance (%)	Cumulative (%)	Primary loading	Secondary loading	Dimension
PC1 Geotechnical instability	2.54	50.8	50.8	InSAR deformation (0.892)	Slope gradient (0.845)	Terrain mass-movement vulnerability

PC2 Ecological degradation	1.18	23.6	74.4	NDVI deficit (0.865)	Forest canopy loss (0.782)	Canopy health trajectory
PC3 Hydrological disturbance	0.65	13.0	87.4	Drainage density (0.764)	Stream proximity (−0.685)	Runoff and gully erosion
PC4 Anthropogenic pressure	0.38	7.6	95.0	Settlement buffer (0.812)	Infrastructure proximity (0.640)	Human encroachment
PC5 Soil quality deficiency	0.25	5.0	100.0	Topsoil loss (−0.725)	Soil organic carbon (0.690)	Pedological recovery capacity

5.6 Correlates and predictors of risk

Composite risk correlates most strongly with InSAR deformation (r = 0.815) and slope (r = 0.742), negatively with mean NDVI (r = −0.684) and soil quality (r = −0.512), and weakly but significantly with population density (r = 0.325) (Table 8; N = 184 plots). Slope and deformation are themselves correlated (r = 0.615), and NDVI tracks soil quality (r = 0.680). These results support H1, H2 and H3.

Table 8. Pearson correlations (N = 184 plots)

Variable	Slope (X1)	Mean NDVI (X2)	InSAR deformation (X3)	Population density (X4)	Soil quality (X5)	Composite risk (Y)
Slope (X1)	1	−0.428**	0.615***	−0.210*	−0.382**	0.742***
Mean NDVI (X2)	−0.428**	1	−0.534***	0.145	0.680***	−0.684***
InSAR deformation (X3)	0.615***	−0.534***	1	−0.092	−0.445**	0.815***
Population density (X4)	−0.210*	0.145	−0.092	1	0.182	0.325**
Soil quality (X5)	−0.382**	0.680***	−0.445**	0.182	1	−0.512***
Composite risk (Y)	0.742***	−0.684***	0.815***	0.325**	−0.512***	1

*Two-tailed: *** $p < 0.001$, ** $p < 0.01$, * $p < 0.05$.*

The regression model explains 78.4% of RRI variance (R = 0.885, $R^2 = 0.784$, adjusted $R^2 = 0.778$; F = 129.45, $p < 0.001$; standard error 4.86; Durbin–Watson 1.942) (Table 9). All five predictors are significant. By standardised effect, InSAR deformation is largest (β = 0.465), then slope (0.312), NDVI deficit (0.285), soil-carbon deficit (0.168) and settlement density (0.124). Each additional mm/yr of subsidence adds 0.42 RRI points and each degree of slope 0.69 points. Collinearity is low (maximum VIF 1.84) and residuals show no autocorrelation.

Table 9. Multiple regression of the Rehabilitation Risk Index

Predictor	B	SE	Standardised β	t	p	VIF
Intercept	14.825	3.120	—	4.752	< 0.001	—

InSAR deformation rate (mm/yr)	0.418	0.042	0.465	9.952	< 0.001	1.624
Slope (°)	0.685	0.088	0.312	7.784	< 0.001	1.842
NDVI deficit (1 − NDVI)	28.450	4.215	0.285	6.750	< 0.001	1.512
Soil organic carbon deficit (%)	4.120	0.945	0.168	4.360	< 0.001	1.385
Settlement density (persons/km²)	0.038	0.011	0.124	3.455	0.001	1.140

5.7 Rehabilitation Risk Index classes

High and critical classes cover 342.8 km², or 23.1% of the landscape (Table 10). They hold 26,200 of the 39,900 exposed residents (65.7%). The critical class alone is 8.4% of the area (124.2 km²) but holds 14,800 people, the largest exposed population of any class, so exposure rises steeply with risk. At the other end, 810.6 km² (54.6%) is very low or low risk.

Table 10. RRI classes, extent and exposure

Class	RRI interval	Area (km²)	Share (%)	Cumulative (%)	Exposed population	Condition
I Very low	0–20	425.4	28.6	28.6	1,850	Stable native forest, negligible deformation
II Low	20.01–40	385.2	25.9	54.6	4,200	Gentle terrain, active farmland, moderate vegetation
III Moderate	40.01–60	332.2	22.4	76.9	7,650	Degraded woodland, moderate slope, minor gullying
IV High	60.01–80	218.6	14.7	91.6	11,400	Steep slopes, vegetation deficit, active soil wash, mining buffer
V Critical	80.01–100	124.2	8.4	100.0	14,800	Active pit highwalls, subsidence above 30 mm/yr, severe contamination
Total	0–100	1,485.6	100.0	100.0	39,900	Full landscape coverage

5.8 Spatial clustering

Risk is strongly clustered (global Moran's I = 0.684, Z = 9.82, p < 0.001), which supports H4 (Table 11). The high-high hotspot covers 268.4 km² with mean RRI 84.6 and is driven by deformation and slope instability. The low-low coldspot covers 482.5 km² of undisturbed dense forest with mean RRI 14.8. Two outlier types need separate handling: 74.3 km² of isolated pits inside stable forest (high-low, mean RRI 68.2) and 62.1 km² of vegetated patches on steep buffers (low-high, 36.5). The remaining 598.3 km² (40.3%) shows no significant pattern.

Table 11. LISA cluster statistics

Cluster	Dominant profile	Mean RRI	Local Moran's I	Z (p)	Area (km²)	Action tier
High-high	Deformation + slope instability	84.6	0.742	8.94 (< 0.001)	268.4	1: Immediate stabilisation

Low-low	Undisturbed dense forest	14.8	0.615	7.12 (< 0.001)	482.5	4: Conservation and monitoring
High-low	Isolated pit in stable forest	68.2	−0.384	−3.85 (< 0.01)	74.3	2: Containment and remediation
Low-high	Vegetated patch on steep buffer	36.5	−0.295	−2.94 (< 0.05)	62.1	3: Selective soil support
Not significant	Mixed farmland and scrub	46.1	0.042	0.58 (> 0.05)	598.3	5: Routine catchment care

5.9 Intervention priorities

Eight management sectors were ranked by RRI and exposed population (Table 12). They cover 35,200 residents, 88% of all exposed people, and have a mean RRI of 65.2. The West Pit Highwall Zone ranks first (RRI 94.2; −48.5 mm/yr; 48° slope; 4,200 people; headwater spring system at stake), then Overburden Spoil Dump #3 (86.8; 5,100 people) and the South Access Corridor cut-slope (76.5; 3,800 people). The North Tailings Embankment ranks fourth on RRI (71.4) but has the largest exposed population among the top four (6,500). The agro-forestry sector has the most people (8,200) but ranks seventh because its risk is low (42.1).

Table 12. Rehabilitation priority ranking

Rank	Sector	RRI	Exposed people	Main risk driver	Asset at stake	Recommended action
1 Critical	West Pit Highwall Zone	94.2	4,200	Subsidence −48.5 mm/yr, 48° slope	Headwater spring system	Bench regrading, sub-horizontal drains, tensile mesh pinning, hydroseeding
2 Critical	Overburden Spoil Dump #3	86.8	5,100	Slope creep −32.8 mm/yr, topsoil deficit	Riparian stream buffer	Terracing, toe rock-buttressing, vetiver bio-fencing, compost bio-capping
3 High	South Access Corridor cut-slope	76.5	3,800	Wedge-failure potential, haul vibration, 42° slope	Settlement transport link	Soil nailing, shotcrete revetment, runoff diversion flumes
4 High	North Tailings Embankment	71.4	6,500	Pore pressure, liquefaction susceptibility	Downstream wetland habitat	Buttress widening, relief wells, automated inclinometer array
5 Moderate	Central Tailings Peripheral Buffer	64.8	2,800	Trace-metal runoff, sparse vegetation (NDVI 0.245)	Agricultural drainage canal	Phytoremediation swales (*Typha latifolia*), biochar conditioning, berms

6 Moderate	Degraded Foot-Slope Scrubland	54.2	3,400	Sheet-wash erosion, overgrazing	Native secondary woodland	Enclosure fencing, rotational grazing, contour trenches, native planting
7 Low	Agro-Forestry Catchment Sector	42.1	8,200	Rill erosion, farm chemical runoff	Groundwater recharge aquifer	Agroforestry hedgerows, mulching, 15 m riparian grass strips
8 Low	Reclaimed Spoil Bench Sector 1	31.5	1,200	Minor settlement, immature root binding	Young afforestation stand	Enrichment planting with nitrogen-fixing legumes, drone NDVI audits
Total	8 sectors	65.2 (mean)	35,200	Multi-hazard	Watershed protection	Phased five-year roadmap, 2026–2030

6. Discussion

6.1 Vegetation recovery does not mean stability

The central result is that two axes of risk run separately. PCA puts geotechnical instability (51% of variance) and ecological degradation (24%) on different components, and the sector data show why. The east reclaimed spoil bench is low-risk and stable (FoS 1.55), but the west pit highwall has a factor of safety of 0.92 and the tailings perimeter has lost vegetation since 1990. A rehabilitation audit that reads only NDVI or plantation counts would rate the first well and miss the second. This is why the AHP puts deformation (0.42) and slope (0.26) above the vegetation deficit (0.10). Slope and deformation also dominate the regression ($\beta = 0.47$ and 0.31).

6.2 Mining expansion and partial recovery

The LULC results are consistent with published evidence of open-cast expansion. Mukherjee and Pahari (2018) report open-cast area growing from 26.15 km² in 1990 to 48.52 km² in 2016, an increase of 22.37 km² or 85.6% (about 2.4% a year). The class used here, mining pits and barren dumps, also includes overburden and barren surfaces, so its areas (94.2 to 182.1 km² by 2020) are larger and not directly comparable, but the direction and timing agree. The reversal after 2020 (−17.6 km²) and the 33.4 km² forest gain are encouraging. Yet 83% of the 1990 mining footprint remained mining or barren land in 2026, and 170.1 km² of forest was lost over the period, much of it to degraded woodland (114.5 km²) rather than directly to mines. The landscape is losing quality faster than it is losing cover.

6.3 Deformation rates and the published record

The highest sector rate here (−48.5 mm/yr, 2020–2026) is more than twice the maximum of −21.18 mm/yr reported for 2017–2023 in a coalfield-wide 2024 Sentinel-1 study. The two are not the same quantity: one is a sector mean on an active highwall, the other a coalfield maximum over an earlier period, and the sectors here are mine-specific slopes. The difference should still be explained with a common reference point, line-of-sight to vertical conversion and ground control before the figure is quoted outside this study. Either way, the direction of the evidence is the same: subsidence is large enough to threaten infrastructure.

6.4 Construction is not rehabilitation

The institutional record shows the same gap between outputs and outcomes. The CAG audit (July 2023 position) found that 7,344 of 10,144 proposed houses for non-ECL families had been built (72.4%), 2,800 (27.6%) were still under construction and only 156 flat owners (2.1% of those built) held provisional possession certificates. A 2025 Parliamentary reply recorded 52 affected families temporarily shifted to available ECL quarters and 186 ECL employees moved to safe quarters, and noted affected stretches of the NH-2 bypass (300 m), DB Road (about 550 m) and the Andal–Sitarampur rail link (100 m and 150 m). These figures come from different dates and categories and must not be added together. They do show that rehabilitation is lived through occupancy, safety, services and livelihoods, which is why the priority ranking here weights exposure as well as hazard.

Financial provision tells a similar story. ECL's site-restoration provision rose from ₹875.60 crore to ₹1,041.35 crore in 2024–25, an increase of ₹165.75 crore (18.9%), comprising an additional provision of ₹135.01 crore and unwinding of discount of ₹48.12 crore, less a withdrawal of ₹17.38 crore. This is a company-wide accounting obligation, not Raniganj spending, and it says nothing about outcomes. Money, physical reclamation, vegetation survival, geological safety and household rehabilitation need to be tracked in one system.

6.5 Hypotheses

- **H1 (deformation and slope) is supported.** Deformation ($r = 0.815$; $\beta = 0.465$) and slope ($r = 0.742$; $\beta = 0.312$) are the strongest correlates and predictors of RRI.
- **H2 (vegetation and soil deficits) is supported.** NDVI is negatively correlated with risk ($r = -0.684$) and NDVI deficit and soil-carbon deficit are significant predictors ($p < 0.001$).
- **H3 (settlement density) is supported, with a small effect.** The correlation is 0.325 and β is 0.124, the smallest of the five predictors.
- **H4 (spatial clustering) is supported.** Moran's I of 0.684 ($Z = 9.82$) and a 268.4 km² hotspot.
- **H5 (integrated index beats single indicators) is supported only in a limited sense.** The five-predictor model explains 78.4% of RRI variance, against 66.4% for the best single indicator (deformation, $r^2 = 0.815^2$). Because the RRI is built from these same indicators, the gain describes the index and does not validate it (Section 8).

6.6 Contribution of the RRI

The RRI stops three common errors. A site with good vegetation but active subsidence is not scored as rehabilitated. A degraded pit far from people is not ranked above a moderately degraded slope above homes. And outliers are not lost in the average: isolated pits in stable forest (74.3 km²) and green patches on steep buffers (62.1 km²) get their own action tiers, which a single risk map would hide.

7. Rehabilitation framework and policy recommendations

Figure -8

7.1 Framework

Action should follow the LISA tiers and the priority ranking: Tier 1 immediate stabilisation of the 268.4 km² hotspot, Tier 2 containment of isolated pits, Tier 3 selective soil support, Tier 4

conservation and monitoring of the 482.5 km² coldspot, and Tier 5 routine care elsewhere. Within each tier the work falls into five strands.

Strand	Intervention	Monitoring indicator
Geological	Void treatment, backfilling, slope engineering, restricted access	Deformation velocity; factor of safety
Overburden	Regrading, terracing, toe buttressing, erosion control	Slope movement; erosion rate
Soil and vegetation	Topsoil replacement, biochar, native planting, phytoremediation	Soil organic carbon, pH; NDVI and survival rate
Water	Mine-water treatment, drainage restoration, wetland protection	pH, TDS, iron, sulphate
Social and economic	Safe relocation, services, livelihood and skills support	Households actually relocated; income and employment recovery
Institutional	GIS-based monitoring and audit	Rehabilitation completion rate

Planting should follow technical stabilisation, with soil preparation and drainage in place first. A phased five-year roadmap (2026–2030) starts with the two critical sectors, whose combined 9,300 residents face the highest hazard, then moves to the high- and moderate-risk sectors, and ends with maintenance of the low-risk sectors.

7.2 Recommendations

1. **Keep a Rehabilitation Risk Register.** Every surface mine holds a GIS register of geological, environmental and social rehabilitation risks, updated each year.
2. **Monitor after closure.** Monitoring continues after backfilling and plantation are complete.
3. **Combine satellite and ground data.** Sentinel-1 deformation is checked against GPS, geological investigation and field survey.
4. **Rank by hazard and exposure.** Investment follows RRI multiplied by exposed population and infrastructure, not hectares reclaimed.
5. **Manage mine water.** Abandoned pits and contaminated drainage are monitored and treated systematically.
6. **Set ecological performance standards.** Plantation success is judged by survival, native species, soil recovery and landscape connectivity.
7. **Coordinate institutions.** ECL, ADDA, CMPDI and the West Bengal Government share one set of responsibilities and one dataset.
8. **Report outcomes, not outputs.** Annual reports separate houses built, possession certificates issued, families actually relocated and livelihoods restored.
9. **Build a common monitoring dashboard.** It shows mine-wise reclamation status, annual vegetation change, deformation alerts, abandoned pit locations, expenditure, settlement exposure and resettlement progress.
10. **Involve communities.** Residents take part in risk mapping, planning and post-relocation monitoring.

8. Limitations

1. **Classification accuracy is not reported.** Overall, producer's and user's accuracy and Kappa for each epoch are needed before the LULC areas in Tables 2 and 3 can be relied on.
2. **Mixed sensors and seasons.** Landsat epochs are dry-season scenes from May–June at 30 m, while the 2026 epoch is a March Sentinel-2 scene at 10 m. Part of the 2020–2026 forest gain and mining decline may reflect resolution and phenology, not land change. Re-running 2026 on a May–June scene resampled to 30 m would test this.

3. **The regression is partly circular.** The RRI is built from the same indicators used as predictors, so the high R^2 (0.784) shows how the index is composed, not how well it predicts outcomes. A stronger test uses independent outcomes such as observed slope failures, vegetation survival or successful resettlement.
4. **PCA specification.** The five eigenvalues sum to 5, which implies five input variables, but ten variables appear in the loadings. The input set and the number of components should be reconciled, and the 100% cumulative variance read as an artefact of retaining all components. The Kaiser rule keeps two.
5. **AHP judgements and sensitivity.** The pairwise comparisons are expert judgements and no sensitivity test of the weights is reported. The consistency ratio shows internal consistency, not correctness.
6. **Deformation validation.** Sentinel-1 rates need atmospheric correction, a stable reference point and ground control (GPS or levelling), and the difference from the −21.18 mm/yr published maximum should be explained.
7. **Vegetation and soils.** NDVI does not measure soil quality, species composition or plantation survival. Seven zones are a small sample of a 1,485.6 km² landscape.
8. **Administrative statistics.** CAG, Parliamentary and ECL figures refer to different dates, populations and accounting categories and are reported side by side, not combined.
9. **Exposure.** Exposed-population counts depend on settlement data and the buffers used to define exposure. Household-level data should be anonymised.

9. Conclusion

The Raniganj landscape shows partial recovery without secure rehabilitation. Between 1990 and 2026, dense forest fell by 133.8 km² and mining pits and dumps grew by 70.3 km², although both reversed after 2020. Vegetation improved where land was deliberately rebuilt, but not on the tailings perimeter or the pit highwall. Geological instability, measured by InSAR deformation and slope, is the strongest driver of risk and is independent of vegetation recovery.

The RRI places 342.8 km² (23.1%) of the landscape and 26,200 residents in high or critical risk, in a spatially clustered pattern (Moran's I = 0.684) with a 268.4 km² hotspot. The West Pit Highwall, Overburden Spoil Dump #3 and the South Access Corridor cut-slope are the first priorities. Published audit and financial records show that construction and provisioning are not the same as safe, occupied, livelihood-restoring rehabilitation.

Rehabilitation in Raniganj should therefore move from reclamation measured by area backfilled or trees planted to risk-based, spatially monitored and socially inclusive rehabilitation, measured by geological stability, ecological recovery, residential safety and restored livelihoods. The limitations above, above all independent validation of the index and of the 2026 epoch, define the next stage of the work.

References

1. Akala, V. A., & Lal, R. (2001). Soil organic carbon pools and sequestration rates in reclaimed minesoils in Ohio. *Journal of Environmental Quality, 30*(6), 2098–2104.

2. Dhar, S. B., & Dutta, M. (2020). Changing land use pattern in the Raniganj coal belt and its sustainable management: A case study of Mangalpur Opencast Colliery. *Current World Environment, 15*(Special Issue 1), 76–88. https://doi.org/10.12944/CWE.15.Special-Issue1.05

3. Ghose, M. K. (2001). Management of topsoil for geo-environmental reclamation of coal mining areas. *Environmental Geology, 40*, 1405–1410.

4. Hossain, S. S., & Chattoraj, K. K. (2022). Evolution of opencast mines in the Raniganj Coalfield (India): An assessment through multi-temporal satellite data. *Journal of the Geological Society of India, 98*(3), 387–394. https://doi.org/10.1007/s12594-022-1990-5

5. Mukherjee, S., & Pahari, D. P. (2023). Opencast coal mining induced land use land cover change: A case study of Pandabeswar block, West Bengal, India through images available from Google Earth. *Transactions of the Institute of Indian Geographers, 45*(2).

6. Sarkar, A. (2018). Accuracy assessment and analysis of land use land cover change using geoinformatics technique in Raniganj coalfield area, India. *International Journal of Environment, Ecology, Family and Urban Studies, 11*(1), 25–34.

7. Sarkar, A. (2019). Land use dynamics and landscape patterns assessment using geoinformatics techniques in Raniganj Coalfield, India. *Research Journal of Science and Technology, 11*(1), 27–37. https://doi.org/10.5958/2349-2988.2019.00004.4

8. Singh, G. (2007). Environmental impact assessment of coal mining and mitigation measures. *Journal of Environmental Management, 86*(2), 362–370.

9. Ripley, E. A., Redmann, R. E., & Crowder, A. A. (1996). *Environmental effects of mining*. St. Lucie Press.

10. Younger, P. L., Banwart, S. A., & Hedin, R. S. (2002). *Mine water: Hydrology, pollution, remediation*. Kluwer Academic Publishers.

11. Congalton, R. G. (1991). A review of assessing the accuracy of classifications of remotely sensed data. *Remote Sensing of Environment, 37*(1), 35–46. https://doi.org/10.1016/0034-4257(91)90048-B

12. Drusch, M., Del Bello, U., Carlier, S., Colin, O., Fernandez, V., Gascon, F., Hoersch, B., Isola, C., Laberinti, P., Martimort, P., Meygret, A., Spoto, F., Sy, O., Marchese, F., & Bargellini, P. (2012). Sentinel-2: ESA's optical high-resolution mission for GMES operational services. *Remote Sensing of Environment, 120*, 25–36. https://doi.org/10.1016/j.rse.2011.11.026

13. Foody, G. M. (2002). Status of land cover classification accuracy assessment. *Remote Sensing of Environment, 80*(1), 185–201. https://doi.org/10.1016/S0034-4257(01)00295-4

14. Huete, A. R. (1988). A soil-adjusted vegetation index (SAVI). *Remote Sensing of Environment, 25*(3), 295–309. https://doi.org/10.1016/0034-4257(88)90106-X

15. Huete, A., Didan, K., Miura, T., Rodriguez, E. P., Gao, X., & Ferreira, L. G. (2002). Overview of the radiometric and biophysical performance of the MODIS vegetation indices. *Remote Sensing of Environment, 83*(1–2), 195–213. https://doi.org/10.1016/S0034-4257(02)00096-2

16. Kennedy, R. E., Yang, Z., & Cohen, W. B. (2010). Detecting trends in forest disturbance and recovery using yearly Landsat time series: 1. LandTrendr—Temporal segmentation algorithms. *Remote Sensing of Environment, 114*(12), 2897–2910. https://doi.org/10.1016/j.rse.2010.07.008

17. Pontius, R. G., Jr., & Millones, M. (2011). Death to Kappa: Birth of quantity disagreement and allocation disagreement for accuracy assessment. *International Journal of Remote Sensing, 32*(15), 4407–4429. https://doi.org/10.1080/01431161.2011.552923

18. Roy, D. P., Wulder, M. A., Loveland, T. R., Woodcock, C. E., Allen, R. G., Anderson, M. C., Helder, D., Irons, J. R., Johnson, D. M., Kennedy, R., Scambos, T. A., Schaaf, C. B., Schott, J. R., Sheng, Y., Vermote, E. F., Belward, A. S., Bindschadler, R., Cohen, W. B., Gao, F., ... Zhu, Z. (2014). Landsat-8: Science and product vision for terrestrial global change research. *Remote Sensing of Environment, 145*, 154–172. https://doi.org/10.1016/j.rse.2014.02.001

19. Rouse, J. W., Jr., Haas, R. H., Schell, J. A., & Deering, D. W. (1974). Monitoring vegetation systems in the Great Plains with ERTS. In *Third Earth Resources Technology Satellite-1 Symposium* (NASA SP-351, Vol. 1, pp. 309–317). NASA.

20. Tucker, C. J. (1979). Red and photographic infrared linear combinations for monitoring vegetation. *Remote Sensing of Environment, 8*(2), 127–150. https://doi.org/10.1016/0034-4257(79)90013-0

21. Bradshaw, A. D. (1997). Restoration of mined lands—Using natural processes. *Ecological Engineering, 8*(4), 255–269.

22. Cooke, J. A., & Johnson, M. S. (2002). Ecological restoration of land with particular reference to the mining of metals and industrial minerals: A review of theory and practice. *Environmental Reviews, 10*(1), 41–71.

23. Harris, J. A., Hobbs, R. J., Higgs, E., & Aronson, J. (2006). Ecological restoration and global climate change. *Restoration Ecology, 14*(2), 170–176.

24. Holl, K. D. (2002). Tropical moist forest restoration. In M. R. Perrow & A. J. Davy (Eds.), *Handbook of ecological restoration* (Vol. 2). Cambridge University Press.

25. Mendez, M. O., & Maier, R. M. (2008). Phytostabilization of mine tailings in arid and semiarid environments—An emerging remediation technology. *Environmental Health Perspectives, 116*(3), 278–283.

26. Prach, K., & Hobbs, R. J. (2008). Spontaneous succession versus technical reclamation in the restoration of disturbed sites. *Restoration Ecology, 16*(3), 363–366.

27. Sheoran, V., Sheoran, A. S., & Poonia, P. (2010). Soil reclamation of abandoned mine land by revegetation: A review. *International Journal of Soil, Sediment and Water, 3*(2), Article 13.

28. Tordoff, G. M., Baker, A. J. M., & Willis, A. J. (2000). Current approaches to the revegetation and reclamation of metalliferous mine wastes. *Chemosphere, 41*(1–2), 219–228.

29. Walker, L. R., Walker, J., & Hobbs, R. J. (Eds.). (2007). *Linking restoration and ecological succession*. Springer.

30. International Council on Mining and Metals. (2019). *Integrated mine closure: Good practice guide* (2nd ed.). ICMM.

31. Carver, S. J. (1991). Integrating multi-criteria evaluation with geographical information systems. *International Journal of Geographical Information Systems, 5*(3), 321–339.

32. Chen, Y., Yu, J., & Khan, S. (2010). Spatial sensitivity analysis of multi-criteria weights in GIS-based land suitability evaluation. *Environmental Modelling & Software, 25*(12), 1582–1591.

33. Eastman, J. R., Jin, W., Kyem, P. A. K., & Toledano, J. (1995). Raster procedures for multi-criteria/multi-objective decisions. *Photogrammetric Engineering & Remote Sensing, 61*(5), 539–547.

34. Feizizadeh, B., & Blaschke, T. (2013). GIS-multicriteria decision analysis for landslide susceptibility mapping: Comparing three methods for the Urmia Lake Basin, Iran. *Natural Hazards, 65*, 2105–2128.

35. Jankowski, P. (1995). Integrating geographical information systems and multiple criteria decision-making methods. *International Journal of Geographical Information Systems, 9*(3), 251–273.

36. Malczewski, J. (1999). *GIS and multicriteria decision analysis*. John Wiley & Sons.

37. Malczewski, J. (2006). GIS-based multicriteria decision analysis: A survey of the literature. *International Journal of Geographical Information Science, 20*(7), 703–726.

38. Saaty, T. L. (1980). *The analytic hierarchy process*. McGraw-Hill.

39. Saaty, T. L. (2008). Decision making with the analytic hierarchy process. *International Journal of Services Sciences, 1*(1), 83–98.

40. Saaty, T. L., & Vargas, L. G. (2012). *Models, methods, concepts & applications of the analytic hierarchy process* (2nd ed.). Springer.

41. Anselin, L. (1995). Local indicators of spatial association—LISA. *Geographical Analysis, 27*(2), 93–115.

42. Brunsdon, C., Fotheringham, A. S., & Charlton, M. (1996). Geographically weighted regression: A method for exploring spatial nonstationarity. *Geographical Analysis, 28*(4), 281–298.

43. Cliff, A. D., & Ord, J. K. (1981). *Spatial processes: Models & applications*. Pion.

44. Fotheringham, A. S., Brunsdon, C., & Charlton, M. (2002). *Geographically weighted regression: The analysis of spatially varying relationships*. John Wiley & Sons.

45. Getis, A., & Ord, J. K. (1992). The analysis of spatial association by use of distance statistics. *Geographical Analysis, 24*(3), 189–206.

46. Hair, J. F., Black, W. C., Babin, B. J., & Anderson, R. E. (2019). *Multivariate data analysis* (8th ed.). Cengage.

47. Jolliffe, I. T. (2002). *Principal component analysis* (2nd ed.). Springer.

48. Moran, P. A. P. (1950). Notes on continuous stochastic phenomena. *Biometrika, 37*(1–2), 17–23.

49. O'Sullivan, D., & Unwin, D. J. (2010). *Geographic information analysis* (2nd ed.). John Wiley & Sons.

50. Voogd, H. (1983). *Multicriteria evaluation for urban and regional planning*. Pion.

Declarations

Funding

No specific funding statement was supplied in the source manuscript. The author should confirm whether the work received external, institutional or project funding and insert the exact grant details, or state that no funding was received.

Competing interests

The author should declare any financial or non-financial competing interests. The source draft does not provide a completed declaration.

Ethics approval and consent to participate

The supplied manuscript describes spatial datasets, sample plots and population exposure estimates but does not clearly state whether primary data were collected from human participants. If household interviews, field questionnaires or identifiable personal data were used, insert the approving ethics committee, approval number and consent procedure. If no human-participant research was undertaken, state this explicitly in accordance with the target journal's policy.

Data availability

The manuscript identifies Landsat, Sentinel-1, Sentinel-2, DEM, drainage, settlement, soil and administrative sources. The author should provide stable repository links or access statements for the processed spatial layers, the 184-plot statistical dataset, the AHP comparison matrix, the PCA input matrix and scripts. If restrictions apply, specify the data that can be shared and the conditions for access.

Author contributions

Prof. (Dr.) Shatrajit Goswami: conceptualisation, methodology, investigation, formal analysis, visualisation and writing—original draft; writing—review and editing. The author should confirm that this statement accurately reflects the actual contributions.

Acknowledgements

I would like to thank Coal India authority, field assistants, data providers and other stakeholders who were supported field access, data acquisition or technical validation and other researchers who enlighten in this research work.